

# Conformational Stability of Cytochrome $b_5$ , Enhanced Green Fluorescent Protein, and Their Fusion Protein Hmwb $_5$ –EGFP

A. V. Yantsevich, A. A. Gilep, and S. A. Usanov\*

*Institute of Bioorganic Chemistry, National Academy of Sciences of Belarus, ul. Kuprevicha 5,  
220141 Minsk, Belarus; fax: 375 (172) 63-7274; E-mail: usanov@iboch.bas-net.by*

Received October 9, 2008

Revision received November 6, 2008

**Abstract**—The conformational stabilities of chimeric protein Hmwb $_5$ –EGFP and its constituents (cytochrome  $b_5$  and enhanced green fluorescent protein) in guanidine hydrochloride solutions are reported in this paper. Intensity of fluorescence of tryptophan residues, intensity of EGFP fluorescence in the visible region, absorbance of cytochrome  $b_5$  heme and EGFP fluorophore, and fluorescence anisotropy were used to follow the unfolding process. Thermodynamic parameters of protein unfolding were obtained using different approaches. The data were analyzed using a two-stage model and a linear extrapolation method. Unfolding of protein molecules was additionally monitored by measuring Stern–Volmer constants for tryptophan fluorescence quenching by acrylamide, cesium, and iodide. The accessibility of tryptophan residues of both components in the fusion molecule is lower than in the separate molecules. The thermodynamic stability of the protein globules in the fusion protein is much lower than in the individual protein molecules in solution, the difference in free energy of unfolding being more considerable for cytochrome  $b_5$  ( $29 \pm 4$  and  $13 \pm 2$  kJ/mol) than for EGFP ( $26 \pm 0.9$  and  $20 \pm 2.7$  kJ/mol). The data indicate that artificial protein fusion can greatly affect total structural stability, and in the case of cytochrome  $b_5$  and EGFP it results in decrease in free energy of transition from native to denatured unfolded form and consequently to decrease in thermodynamic stability of protein globules compared to the separate proteins.

DOI: 10.1134/S000629790905006X

**Key words:** microsomal cytochrome  $b_5$ , green fluorescent protein, fluorescence, folding, conformational stability

Thermodynamic stability of multidomain proteins and proteins artificially fused into a single polypeptide chain is of a great significance since understanding peculiarities accompanying joining of the protein globules into one polypeptide chain allows us to envisage behavior of such complex systems, with further their directed modification, to get stable and active enzyme complexes. There are some examples demonstrating that recombinant fusion proteins have much higher expression level in *Escherichia coli* cells. Thus, extremely high expression level for chimeric protein containing cytochrome  $b_5$  and NADH-cytochrome  $b_5$  reductase, cytochrome  $b_5$  and NADPH-cytochrome P450 reductase, in some cases demonstrating high catalytic activity, has been reported [1–3]. One possible reason for such discovered regularities might be increase in thermodynamic stability of such fusion proteins. Careful comparative analysis of thermodynamic stability of these naturally occurring multidomain proteins (cytochrome P450 BM3 (CYP102A1) from

*Bacillus megaterium*, NO-synthase) and separate domains has not been done. However, there are some data indicating that individual domains of CYP102A1 in the content of the holoenzyme cause a very weak mutual stabilizing effect on the structure, and the heme-binding domain is much more stable than the flavin domain [4]. There are some interesting data on engineering a thermostable fatty acid hydroxylase from CYP102A1 by replacing its reductase domain with a more stable reductase domain of CYP102A3 from *Bacillus subtilis* [5].

Cytochrome  $b_5$  is a membrane-bound heme protein consisting of two domains [6, 7]. The N-terminal hydrophilic domain with molecular weight 12,000 Da contains heme, while the C-terminal domain with molecular weight 3000 Da is hydrophobic and serves as a membrane anchor [8]. Cytochrome  $b_5$  participates in the reactions of desaturation and oxidation of fatty acids [9], reduction of methemoglobin in erythrocytes [10], hydroxylation of N-acetylneuraminic acid [11], as well as in microsomal monooxygenase reactions catalyzed by cytochrome P450 [12–14]. The stimulating effect of

\* To whom correspondence should be addressed.

cytochrome  $b_5$  has been shown for some important reactions catalyzed by cytochrome P450, including detoxification of xenobiotics and biosynthesis and degradation of steroid hormones, prostaglandins, leukotrienes, bile acids and vitamin D<sub>3</sub> [15]. However, the molecular mechanisms of the modulating effect of cytochrome  $b_5$  on cytochrome P450 catalyzed reactions are still not clear [16, 17]. Therefore, there is clear interest in elucidation of the intrinsic mechanism of interaction of cytochrome  $b_5$  with cytochrome P450 and NADPH-cytochrome P450 reductase.

We recently engineered an artificial chimeric protein based on full-length rat liver microsomal cytochrome  $b_5$  (134 amino acids) and a mutant form of green fluorescent protein (EGFP, 238 amino acids) [18]. Despite the fact that the spectral properties of the engineered protein correspond to that of the individual proteins, conformation and stability of the domains in the chimeric protein might be different. The changes in thermodynamic stability of protein globules after their inclusion into a fusion protein represents not only fundamental, but also significant practical interest, since the knowledge of regularities of changes in the properties of individual proteins on their fusion into the single polypeptide chain is important for applied enzymology, genetic engineering, and understanding of directed protein evolution.

In the present work, we have carefully analyzed stability of the individual protein globules in the chimeric protein and compared these parameters with those of the separate proteins. The chosen proteins contain specific internal labels (tryptophan, heme, *p*-hydroxybenzylidene imidazolinone), and the changes in spectral properties of these groups were used to follow the process of denaturation of each individual protein separately. The results of the present work indicate that joining of cytochrome  $b_5$  and EGFP into a single polypeptide chain decreases the free energy of transition from native to unfolded form, and consequently, decreases thermodynamic stability of the protein globules as compared to the separate proteins.

## MATERIALS AND METHODS

In the present work we used following chemicals and reagents: guanidine hydrochloride (Merck, Germany), DEAE-cellulose DE52 (Whatman, USA), tryptone, peptone, yeast extract (Difco, USA), phenylmethylsulfonyl fluoride, isopropyl- $\beta$ -D-thiogalactopyranoside (BRL, USA), as well as other chemicals from Sigma (USA). The affinity matrix Ni-IDA-Sepharose 6B was synthesized as previously described [19].

**Preparation of recombinant proteins.** Chimeric recombinant protein Hmwb<sub>5</sub>-EGFP was prepared as previously described [18]. Recombinant rat liver cytochrome  $b_5$  was expressed and purified using metal-affinity chromatography as previously described [20].

Green fluorescent protein (EGFP, mutant form F64L, S65T) [21] was expressed in *E. coli* BL21 cells using expression plasmid pRSET-B under T7 promoter and contained at the N-terminal sequence additional six histidine residues, that allowed quick and efficient purification of the recombinant protein by metal-affinity chromatography using Ni-IDA-Sepharose 6B, with subsequent anion-exchange chromatography on DEAE-cellulose (DE52). The concentration of cytochrome  $b_5$  was determined using molar extinction coefficient  $\epsilon_{413} = 117 \text{ mM}^{-1} \cdot \text{cm}^{-1}$  for the oxidized form of cytochrome  $b_5$  and  $\epsilon_{490} = 56 \text{ mM}^{-1} \cdot \text{cm}^{-1}$  for EGFP. The purity of protein preparations was checked by SDS-PAGE [22].

**Determination of free energy of unfolding of the protein globule.** To determine the free energy of unfolding for the protein molecule, we used as an approximation a two-step model presuming the existence of the protein only in two forms – native and denatured. The protein samples (0.5  $\mu\text{M}$  final protein concentration) in 20 mM sodium phosphate buffer containing guanidine hydrochloride at desired concentrations were incubated for 96 h at 20°C to reach thermodynamic equilibrium. Then tryptophan fluorescence emission spectra ( $\lambda_{\text{ex}} = 297 \text{ nm}$ ), absorption spectra (350–530 nm), and fluorescence anisotropy ( $\lambda_{\text{ex}} = 297 \text{ nm}$ ,  $\lambda_{\text{em}} = 320\text{--}370 \text{ nm}$ ) were measured for each sample. For Hmwb<sub>5</sub>-EGFP and EGFP, EGFP fluorescence emission spectra ( $\lambda_{\text{ex}} = 490 \text{ nm}$ ) were also recorded, and steady state anisotropy was calculated ( $\lambda_{\text{ex}} = 490 \text{ nm}$ ,  $\lambda_{\text{em}} = 500\text{--}520 \text{ nm}$ ).

The equilibrium constant  $K_{U/N}$  for the process  $N \leftrightarrow U$  was calculated according to equation:

$$K_{U/N} = \frac{S_N - S}{S - S_U}, \quad (1)$$

where  $K_{U/N}$  is the equilibrium constant for the process;  $S_N$  is the intensity of the signal of the native form of the protein;  $S$  is the intensity of the signal of the mixture of native and denatured forms;  $S_U$  is the intensity of the signal of the denatured form of the protein.

The signal in this case represents the intensity of fluorescence, absorption, and fluorescence anisotropy. From the plots of the dependence of signal intensity on concentration of denaturant, the concentration of guanidine hydrochloride at which half of the maximum signal intensity change takes place ( $[\text{GuHCl}]_{1/2}$ ) was determined. To determine the free energy of protein denaturation, seven points closed to  $[\text{GuHCl}]_{1/2}$  were chosen. The free energy of transition was calculated according to equation:

$$\Delta G_{[\text{GuHCl}]} = -RT \ln(K_{U/N}), \quad (2)$$

where  $\Delta G_{[\text{GuHCl}]}$  is the free energy of the  $N \leftrightarrow U$  transition at the indicated concentration of guanidine hydrochloride.

ride;  $R$  is the universal gas constant, J/(mol·K);  $T$  is the thermodynamic temperature, K.

Free energy of the  $N \leftrightarrow U$  transition in water solutions was calculated by linear extrapolation [23]. The plot of the dependence of  $\Delta G$  on  $[GuHCl]$  was approximated by the least-squares method to Eq. (3) and the values of  $\Delta G_{[H_2O]}$  and  $m$  were determined:

$$\Delta G_{[GuHCl]}^0 = \Delta G_{[H_2O]} - m[GuHCl], \quad (3)$$

where  $\Delta G_{[GuHCl]}$  is the free energy of the  $N \leftrightarrow U$  transition at the indicated concentration of guanidine hydrochloride, found from Eq. (2), J/mol;  $\Delta G_{[H_2O]}$  is the free energy of the  $N \leftrightarrow U$  transition in water solution, J/mol;  $m$  is a parameter characterizing the "sensitivity" of the molecule to the effect of the denaturing agent, J/mol per mol  $[GuHCl]$ ;  $[GuHCl]$  is the concentration of guanidine hydrochloride, M.

When calculating equilibrium constants for denaturing process using tryptophan steady-state fluorescence anisotropy as a parameter, the data were corrected for changes in quantum yield under exposure of tryptophan residues to the solvent due to protein denaturation [24]. Due to different quantum yields for tryptophan in native and denatured forms of the proteins, to calculate molar contribution of states we use a non-linear approximation of anisotropy according to [24]. In calculations, the quantum yields of tryptophan residues for native and denatured forms of protein were used.

**Determination of Stern–Volmer constants.** To determine the constants of concentration-dependent tryptophan fluorescence quenching, to 0.5  $\mu$ M protein solutions in 20 mM potassium phosphate buffer, pH 7.4, different concentrations of guanidine hydrochloride were added. When using iodide as a quencher, the solution also contained 5 mM potassium thiosulfate to reduce iodine formed on photodecomposition of iodide. The reaction mixture was placed in a fluorometric cell, and the fluorescence spectrum was recorded ( $\lambda_{ex} = 297$  nm,  $\lambda_{em} = 305$ –400 nm). The quencher (2 M acrylamide, 0.5 M  $Cs_2SO_4$ , or 2 M KI) was added to the protein solution, and the emission fluorescence spectrum was recorded. To avoid the effect of dilution, the total volume of quencher did not exceed 10% of the initial volume of the protein solution. The recorded spectra were corrected with respect to dilution and the internal filter effect using the equation:

$$I_{real} = I_{obs} \frac{V}{V_{init}} 10^{\left( \frac{Q\varepsilon_{ex}}{2} + \frac{Q\varepsilon_{em}}{2} \right)}, \quad (4)$$

where  $I_{real}$  is the corrected value of fluorescence intensity, relative units;  $I_{obs}$  is the observed value of fluorescence intensity, relative units;  $V_{init}$  is the initial volume of protein solution, ml;  $V$  is the current volume of protein solution, ml;  $Q$  is the concentration of quencher, M;  $\varepsilon_{ex}$  is

the molar extinction coefficient of quencher at wavelength 297 nm,  $M^{-1}\cdot cm^{-1}$ ;  $\varepsilon_{em}$  is the molar extinction coefficient of quencher at wavelength of emission,  $M^{-1}\cdot cm^{-1}$ .

The fluorescence intensity was determined from the fluorescence emission spectra at wavelength 330 and 350 nm, and plotted dependence of  $I_0/I$  on quencher concentration (acrylamide,  $Cs^+$ , or  $I^-$ ). To determine Stern–Volmer constants, the plots obtained by least squares were approximated by the equation:

$$\frac{I_0}{I} = 1 + k_{sv}[Q], \quad (5)$$

where  $I_0$  is the fluorescence intensity in the absence of quencher;  $I$  is the fluorescence intensity at a particular concentration of quencher  $[Q]$ ;  $k_{sv}$  is the Stern–Volmer constant.

As a control, to assess the effects caused by increasing ionic strength of solution, for every case an experiment was performed with 0.5 M solution of  $Na_2SO_4$  and 2 M solution of KCl.

**Determination of fluorescence anisotropy.** Steady-state anisotropy of protein tryptophan fluorescence was calculated from fluorescence spectra ( $\lambda_{ex} = 297$  nm,  $\lambda_{em} = 320$ –370 nm), obtained for four positions of polarizers of excitation and emission by using following equation:

$$A = \frac{I_{vv} - kI_{vh}}{I_{vv} + 2kI_{vh}}, \quad (6)$$

where  $A$  is the fluorescence anisotropy;  $I_{vv}$  is the intensity of parallel polarized component of fluorescence under vertical polarization of excitation light;  $I_{vh}$  is the intensity of perpendicular polarized component of fluorescence under vertical polarization of excitation light;  $k$  is the gauge factor,

$$k = \frac{I_{hv}}{I_{hh}}, \quad (7)$$

where  $I_{hv}$  is the intensity of vertically polarized component of fluorescence under horizontal polarization of excitation light;  $I_{hh}$  is the intensity of horizontal polarized component of fluorescence under horizontal polarization of excitation light.

All measurements were made at 20°C. For calculations and plotting of graphical illustrations, we used the OriginPro 7.5 program (OriginLab Corporation).

## RESULTS AND DISCUSSION

There are several experimental approaches that can be used to follow protein polypeptide chain unfolding

[25]. To follow the process of polypeptide chain unfolding for separate and chimeric protein cytochrome  $b_5$ , we used in the present work absorption and fluorescence spectroscopy as well as polarized fluorescence. The molar extinction coefficient of heme coordinated by histidine residues in cytochrome  $b_5$  has a significant value of  $117 \text{ mM}^{-1}\cdot\text{cm}^{-1}$  in the Soret region. During protein denaturation and breakdown of coordination bonds, dramatic decrease in molar extinction coefficient at 413 nm to  $40 \text{ mM}^{-1}\cdot\text{cm}^{-1}$  and simultaneous shift of the absorbance maximum to 400 nm takes place (Fig. 1c). Thus, the equilibrium constant for this process can be calculated using Eq. (1), where intensity of the signal is the absorption of the heme protein in the Soret region.

The full-length rat liver cytochrome  $b_5$  contains four tryptophan residues, one of which is located in the hydrophilic domain (Trp27) (Fig. 1a), while three other residues are in the hydrophobic domain (Trp109, Trp110, Trp113). Fluorescence emission spectra of tryptophan residues of cytochrome  $b_5$  at different concentrations of chaotropic agent are shown in Fig. 1b. The quantum yield

of tryptophan fluorescence is sharply decreased due to singlet–singlet energy transfer to heme of cytochrome  $b_5$ , and fluorescence intensity dramatically increases under heme dissociation that takes place in the process of heme protein denaturing. Careful analysis of fluorescence emission spectra of tryptophan residues indicates that denaturing of cytochrome  $b_5$  occurs in at least in two steps. The initial decrease in fluorescence intensity is connected with destabilization of the hydrophobic domain and additional decrease in fluorescence quantum yield of tryptophan residues of the hydrophobic domain. The subsequent increase in fluorescence intensity is connected with heme dissociation and decrease in efficiency of energy transfer.

Anisotropy of intrinsic fluorescence of cytochrome  $b_5$  can be used to differentiate tryptophan residues of two domains of cytochrome  $b_5$ . Fluorophores in different microenvironments have different fluorescence maxima, and as a result relatively accessible to solvent tryptophan residues of hydrophobic domain have a red-shifted maximum in the fluorescence emission spectrum. As a result,

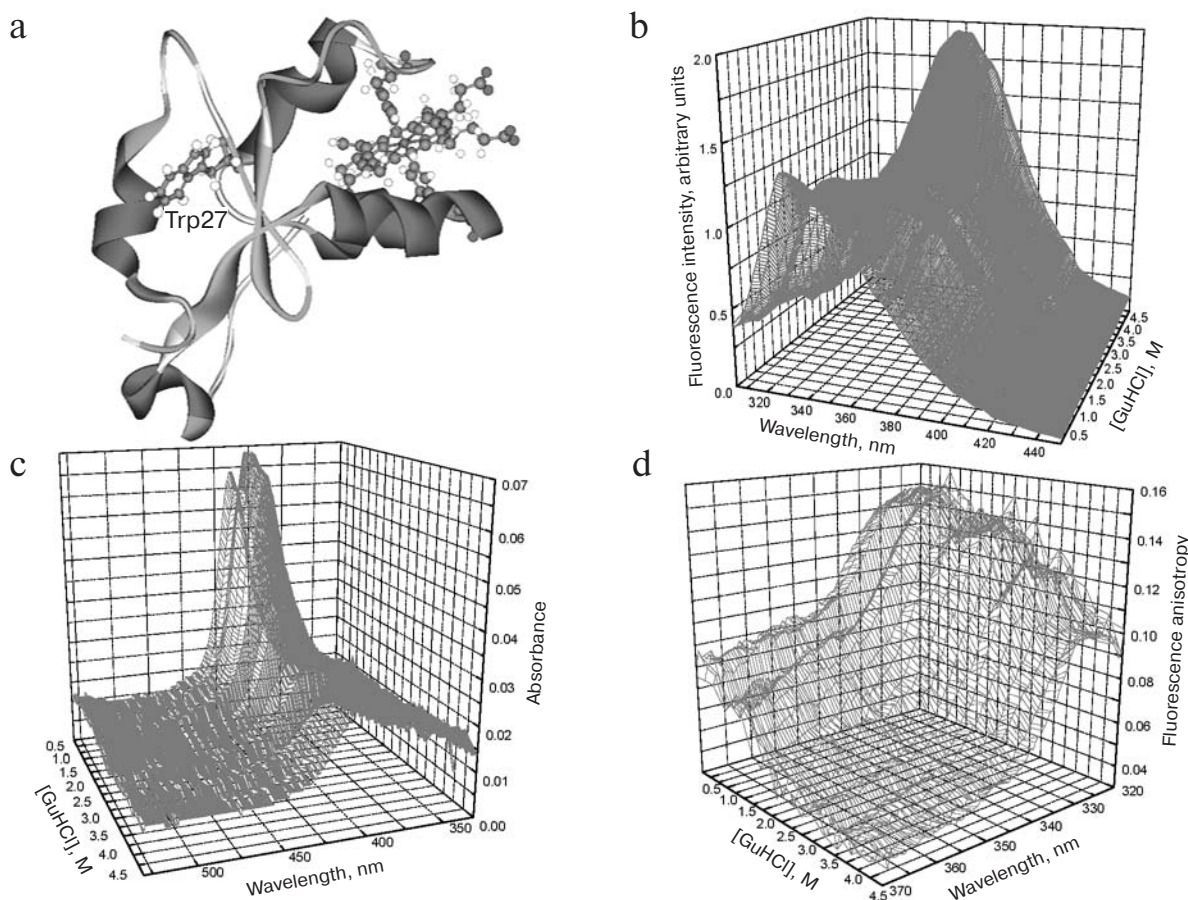


**Fig. 1.** a) Tertiary structure of the hydrophilic domain of rat liver cytochrome  $b_5$  (indicated are the single Trp27 and heme coordinated by His39 and His63 residues); b) fluorescence emission spectra of tryptophan residues; c, d) absorption spectra in the Soret region (c) and spectra of fluorescence anisotropy of tryptophan residues (d) of cytochrome  $b_5$  at different concentrations of guanidine hydrochloride.



steady-state fluorescence anisotropy in the region 330 nm has a value 0.15, and linearly decreases in the region 335–345 nm to 0.1 (Fig. 1d). Denaturing of cytochrome  $b_5$  is followed by decrease in fluorescence anisotropy to 0.11 and 0.05 at wavelengths 330 and 350 nm, respectively. Fluorescence anisotropy at wavelengths 330 and 360 nm is still different, indicating different mobility of tryptophan residues in the denatured heme protein. These parameters were used to calculate the free energy of unfolding of the heme protein molecule. The free energy of transition, parameter  $m$ , and mean point of transition  $[\text{GuHCl}]_{1/2}$  are shown in Table 1 (the omissions are left in that cases when changes in parameters have very small amplitude and do not allow accurate calculation).

The most accurate reflection of the stability of hydrophobic domain of cytochrome  $b_5$  appears to be the data on the changes in the absorption spectra, although in this case it is not possible to observe the two-step nature of the transition. On the other hand, the fluorescence anisotropy shows that the hydrophobic and hydrophilic domains of cytochrome  $b_5$  unfold sequentially. These results are in accordance with the literature data on the mechanism of denaturation of bovine cytochrome  $b_5$ . The free energy of unfolding of the polypeptide chain of microsomal cytochrome  $b_5$ , determined earlier [26], is of

26.5 kJ/mol. For the apo-form of microsomal cytochrome  $b_5$ , the value is  $11.6 \pm 1.5$  kJ/mol [27, 28]. The free energy of transition for recombinant rat liver microsomal cytochrome  $b_5$  is  $29 \pm 4$  kJ/mol.

It is interesting to note an observation made during purification of cytochrome  $b_5$  from inclusion bodies formed under specific conditions of hyperexpression of recombinant cytochrome  $b_5$  in *E. coli* cells. During purification of the apo-form of cytochrome  $b_5$  in denaturing conditions (8 M urea) with subsequent refolding by means of slow dilution or dialysis, the heme protein practically completely precipitates on reaching the concentration of chaotropic agent 2 M. In this case, when heme is preliminarily added to the apo-protein before dialysis, refolding proceeds normally to form soluble holocytochrome  $b_5$ . A possible reason for this phenomenon might be that heme serves as a nucleation center around which normally folded protein is formed.

The denaturation of EGFP was following using four parameters: tryptophan fluorescence intensity ( $\lambda_{\text{ex}} = 297$  nm) (Fig. 2b), steady-state tryptophan fluorescence anisotropy (Fig. 2d), absorption at wavelength 490 nm (Fig. 2c), and fluorescence intensity in the visible region ( $\lambda_{\text{ex}} = 490$  nm,  $\lambda_{\text{em}}^{\text{max}} = 510$  nm) (Fig. 2a). The mutant form of EGFP contains the single tryptophan residue Trp57, so

**Table 1.** Thermodynamic parameters for unfolding of native cytochrome  $b_5$  and EGFP and also cytochrome  $b_5$  and EGFP in the chimeric protein

Characteristic	$\Delta G_0$ , kJ/mol	$m$ , kJ/mol <sup>2</sup>	$[\text{GuHCl}]_{1/2}$ , M	$\Delta G_0$ , kJ/mol	$m$ , kJ/mol <sup>2</sup>	$[\text{GuHCl}]_{1/2}$ , M
cytochrome $b_5$			cytochrome $b_5$ in Hmwb <sub>5</sub> –EGFP			
Absorbance 413 nm	$29 \pm 4$	$14 \pm 1.8$	2	$13 \pm 2$	$7 \pm 1.2$	1.75
Intensity 330 nm	—	—	—	$9 \pm 1$	$6 \pm 0.6$	1.5
350 nm	$35 \pm 6$	$13 \pm 1.6$	2.5	—	—	—
Anisotropy 331 nm	—	—	—	$8.2 \pm 0.7$	$3.6 \pm 0.3$	2.3
350 nm	$8 \pm 0.3$	$4.5 \pm 0.2$	1.75	$8.6 \pm 0.4$	$4.3 \pm 0.1$	2
EGFP			EGFP in Hmwb <sub>5</sub> –EGFP			
Absorbance 490 nm	$27.2 \pm 0.2$	$4 \pm 0.1$	2.75	$21 \pm 0.8$	$5 \pm 0.3$	2.5
Intensity 510 nm	$26 \pm 0.9$	$9.3 \pm 0.3$	2.75	$20 \pm 2.7$	$8 \pm 1$	2.5
330 nm	$4.5 \pm 0.4$	$4.1 \pm 0.5$	1	$9 \pm 1$	$6 \pm 0.6$	1.5
350 nm	$2.1 \pm 0.2$	$2.5 \pm 0.1$	0.8	—	—	—
Anisotropy 331 nm	$14.3 \pm 0.3$	$5.9 \pm 0.2$	2.5	$8.2 \pm 0.7$	$3.6 \pm 0.3$	2.3
350 nm	$12.1 \pm 0.3$	$5.5 \pm 0.1$	2.25	$8.6 \pm 0.4$	$4.3 \pm 0.1$	2

Note: Dashes designate cases when changes of the parameters were not significant enough to make calculations with sufficient precision.

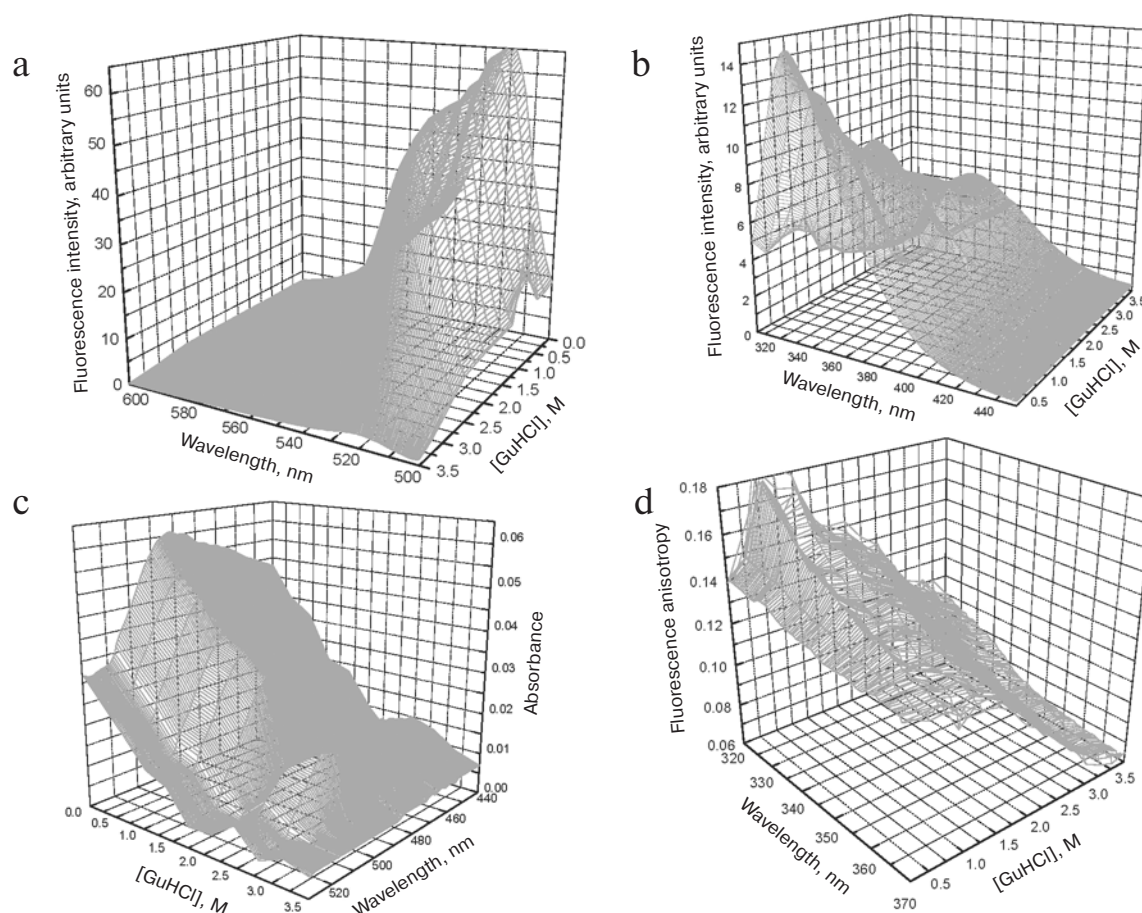


**Fig. 2.** Fluorescence emission spectra in the visible region (a), fluorescence emission spectra of tryptophan residues (b), absorption spectra (c), and intrinsic fluorescence anisotropy (d) of EGFP at different concentrations of guanidine hydrochloride.

monitoring is performed at the level of a single fluorescent marker. The maximum of the fluorescence emission spectrum of the protein is at 331 nm. In the process of denaturation, the quantum yield of fluorescence decreases, which results in a decrease in fluorescence intensity and simultaneous shift of the maximum to 350 nm.

The steady-state tryptophan fluorescence anisotropy of EGFP decreased during protein unfolding from 0.15 to 0.09 at wavelength 331 nm. The changes in the absorption spectrum during protein denaturing are reflected in disappearance of the peak at 490 nm. Exposure of protein fluorophore to solvent molecule decreases fluorescence quantum yield from 0.6 to 0.001 [21]. As a result, fluorescence intensity decreased to the level of noise, while the wavelength maximum in the spectrum did not change. Fluorescence anisotropy of the proteins in the visible region does not change, indicating the absence in denatured protein fluorescent form of fluorophore. Being a relative parameter not dependent from fluorophore concentration, fluorescence anisotropy cannot quantitatively reflect the mole fraction of denatured and native proteins

if their quantum yield is significantly different. Thermodynamic parameters of the denaturing of the protein obtained by linear extrapolation of data of different types are presented in Table 1. Many different mutant forms of green fluorescent protein have been prepared, but studies of thermodynamic stability have not been done for all of them. There are some indications of the presence of a high energy barrier in the process of denaturing of one such form of the protein. Also, a relatively stable intermediate was found [29]. It is necessary to stress the special role of the chromophore of GFP-like proteins for the processes of denaturing and folding. As shown recently, the presence of the chromophore in the central  $\alpha$ -helix results in a reversible process of protein folding–refolding with hysteresis, which disappears after a relatively prolonged time [30]. The chromophore formation closes the structure formed into a deep potential hole with high energetic barrier and is one reason for high protein stability [30] despite a small value of changes in free energy of transition between native and denatured forms [29].

Concerning the denaturing of the chimeric protein, one can suggest that this process is realized independently for each globule forming the chimeric protein. The unfolding process of each of the components of the chimeric protein can be monitored independently. For cytochrome  $b_5$ , the parameter of monitoring is changes in absorbance at 413 nm (Fig. 3c), while for EGFP it is absorbance at 490 nm (Fig. 3c) and fluorescence intensity at the maximum of the emission spectrum with  $\lambda_{\text{ex}} = 490$  nm (Fig. 3a).

Tryptophan fluorescence intensity (Fig. 3b) and anisotropy (Fig. 3d) in chimeric proteins are formed as a sum of these parameters of the individual proteins and separating them precisely is difficult, and therefore calculations have been done formally. The intensity of intrinsic fluorescence of the chimeric protein at increasing guanidine hydrochloride concentration initially decreases even more significantly than in the case of individual cytochrome  $b_5$ , which appears to be due to the contribution of the single tryptophan of EGFP. The subsequent increase in fluorescence intensity, accompanied by shift of the fluorescence maximum to 354 nm, is connected with denaturing of the hydrophilic domain of cytochrome  $b_5$  and heme dissociation.

The curves of unfolding of cytochrome  $b_5$ , EGFP, and Hmwb $_5$ -EGFP are shown in the Figs. 4 and 5. The results of calculations of thermodynamic parameters for the unfolding of individual components of chimeric protein Hmwb $_5$ -EGFP are shown in Table 1. From these data it follows that the values of free energy of denaturation for individual components in the content of the fusion protein are significantly lower than the same parameters for the separate proteins. The free energy for cytochrome  $b_5$  unfolding in the content of the chimeric protein is  $13 \pm 2$  kJ/mol, which is close to the stability of the apo-form of cytochrome  $b_5$ . As concerns EGFP, the  $\Delta G$  decreases from  $26 \pm 0.9$  to  $20 \pm 2.7$  kJ/mol. These results indicate decrease in thermodynamic stability of Hmwb $_5$  and EGFP on joining them into the fusion protein, which is much more reflected in the conformational stability of cytochrome  $b_5$ . The reason for such behavior might be steric modification of some elements of the secondary and tertiary structure of the proteins as a result of mutual effects of protein globules connected by the relatively short Ser-Thr linker.

To get information on accessibility of tryptophan residues to the solvent, we determined the concentration

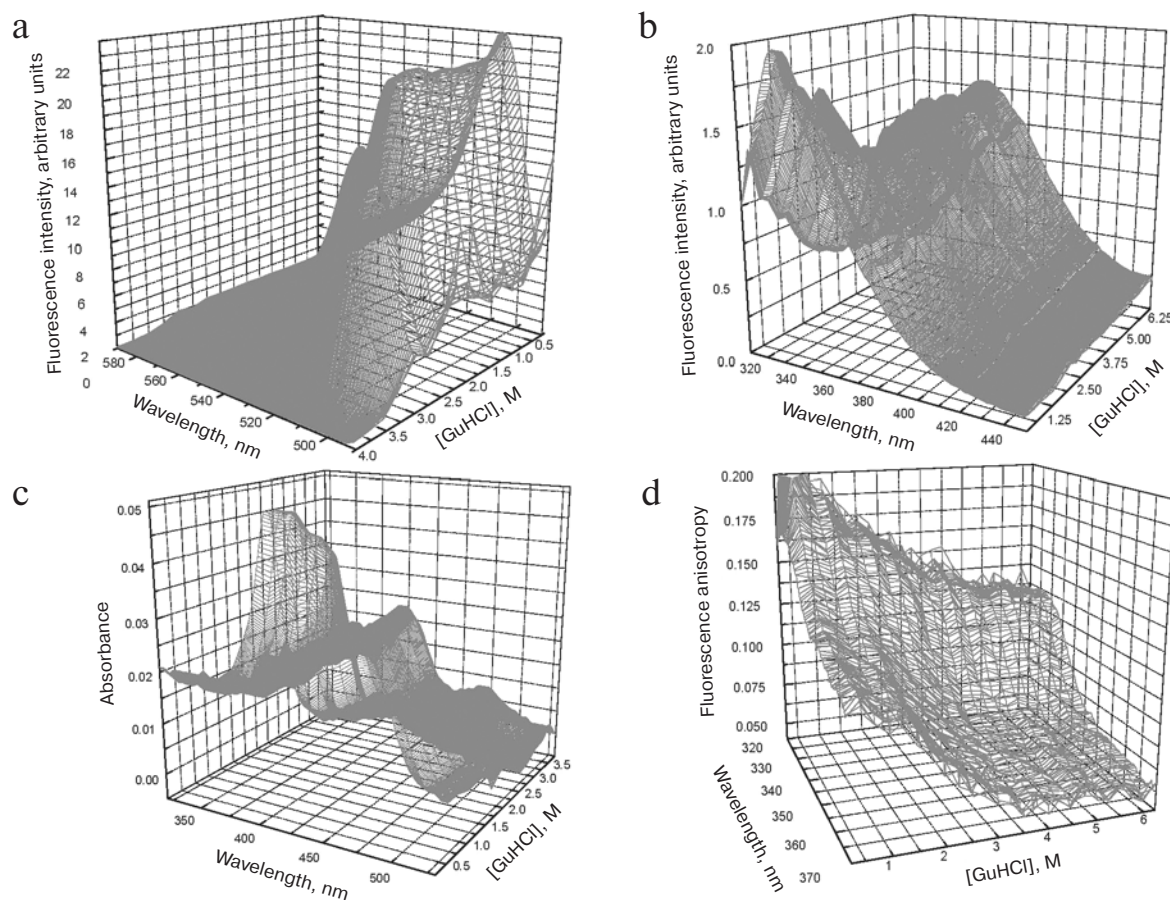


**Fig. 3.** Fluorescence emission spectra in the visible region (a), fluorescence emission spectra of tryptophan residues (b), absorption spectra (c), and intrinsic fluorescence anisotropy (d) of chimeric protein Hmwb $_5$ -EGFP at different concentrations of guanidine hydrochloride.

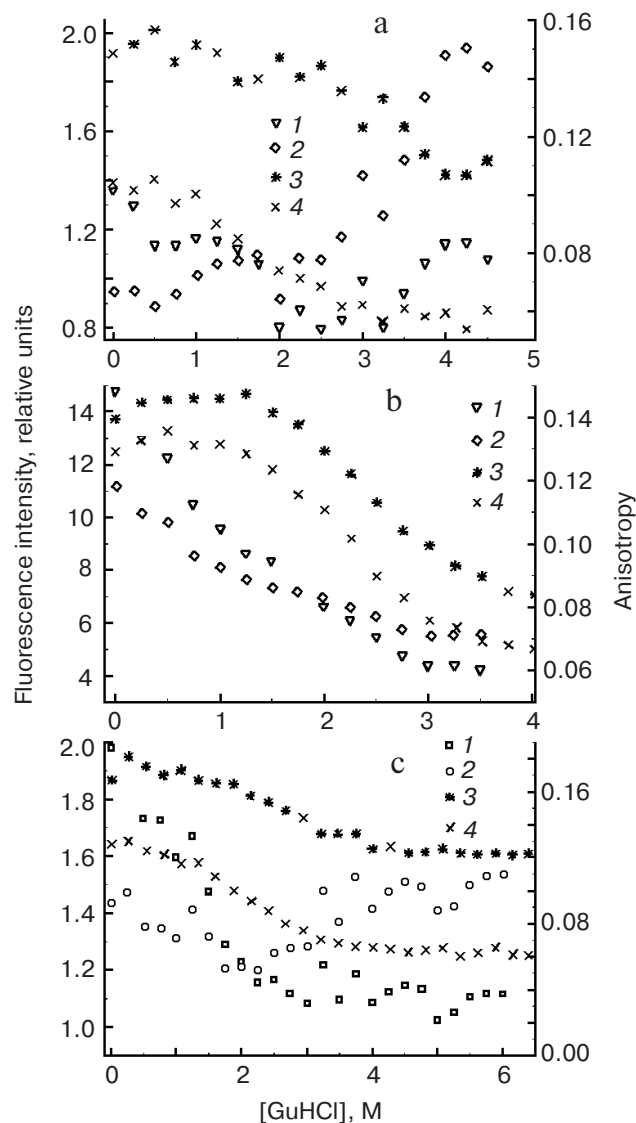


**Fig. 4.** Dependence of fluorescence intensity (1, 2) and anisotropy (3, 4) of tryptophan residues of cytochrome  $b_5$  (a), EGFP (b), and Hmwb<sub>5</sub>-EGFP (c) at 331 and 360 nm, respectively, on concentration of guanidinium hydrochloride.

dependent constants for tryptophan fluorescence quenching (Stern–Volmer constants) using different types of quenchers for native and completely denatured forms of the proteins. We used quenchers having net negative or positive charge or not having any charge at all (acrylamide,  $I^-$  anion,  $Cs^+$  cation). The results obtained on tryptophan fluorescence quenching are presented in Table 2. Control experiments on the effect of the corresponding anion and changes in ionic strength did not show any evident effects. It is necessary to stress that at low ionic strength the charge of quencher can cause large effect on the value of the Stern–Volmer constants due to interaction of quencher charge with local fluorophore microenvironment. For that reason, the constants of

quenching for native protein were determined in buffer with low ionic strength (50 mM Tris-HCl, pH 7.4). Guanidine hydrochloride, being a strong electrolyte, at high concentrations may cause a shielding effect and result in decrease in the value of the bimolecular rate constants of collision.

The different values of the Stern–Volmer constants calculated at two different wavelengths confirm the presence of several groups of tryptophan residues having different accessibility to quencher molecules. As follows from Table 2, tryptophan residues of cytochrome  $b_5$  have indeed different accessibility to quencher since quencher constants determined at 330 and 350 nm have different values. As for EGFP, the presence of the single tryptophan residue is in accordance with similar Stern–Volmer constant values at the two different wavelengths. The following regularity is observed for all types of quenchers: The Stern–Volmer constant for cytochrome  $b_5$  is less than that for EGFP, but higher than that for the chimeric protein. A possible reason for this phenomenon might be shielding of the sites of the quencher access on both proteins after their joining into a single polypeptide chain. Localization and the degree of exposure of tryptophan residues for both proteins are shown in Fig. 6. Despite the fact that, as follows from the tertiary structure of hydrophilic cytochrome  $b_5$ , tryptophan is more exposed than in the model of tertiary structure of GFP, the constants for GFP have larger value. However, it is important to remember that the model of the tertiary structure known for cytochrome  $b_5$  is the model of the hydrophilic domain only, while the structure of the full-length heme protein might be different.

Thus, in the present work we analyzed in detail the changes in parameters observed by absorption and fluo-

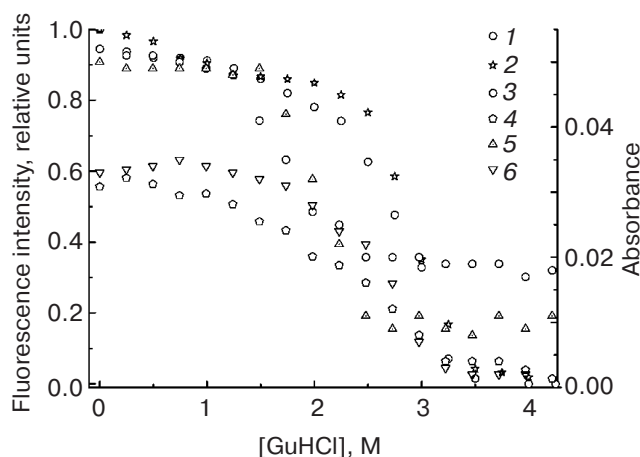


**Fig. 5.** Dependence of fluorescence intensity in the visible region (1, 2), absorbance at 490 nm (3, 4) for EGFP and chimeric protein Hmwb<sub>5</sub>-EGFP, respectively, as well as absorbance at 413 nm for cytochrome  $b_5$  (5) and chimeric protein Hmwb<sub>5</sub>-EGFP (6) on concentration of guanidinium hydrochloride.



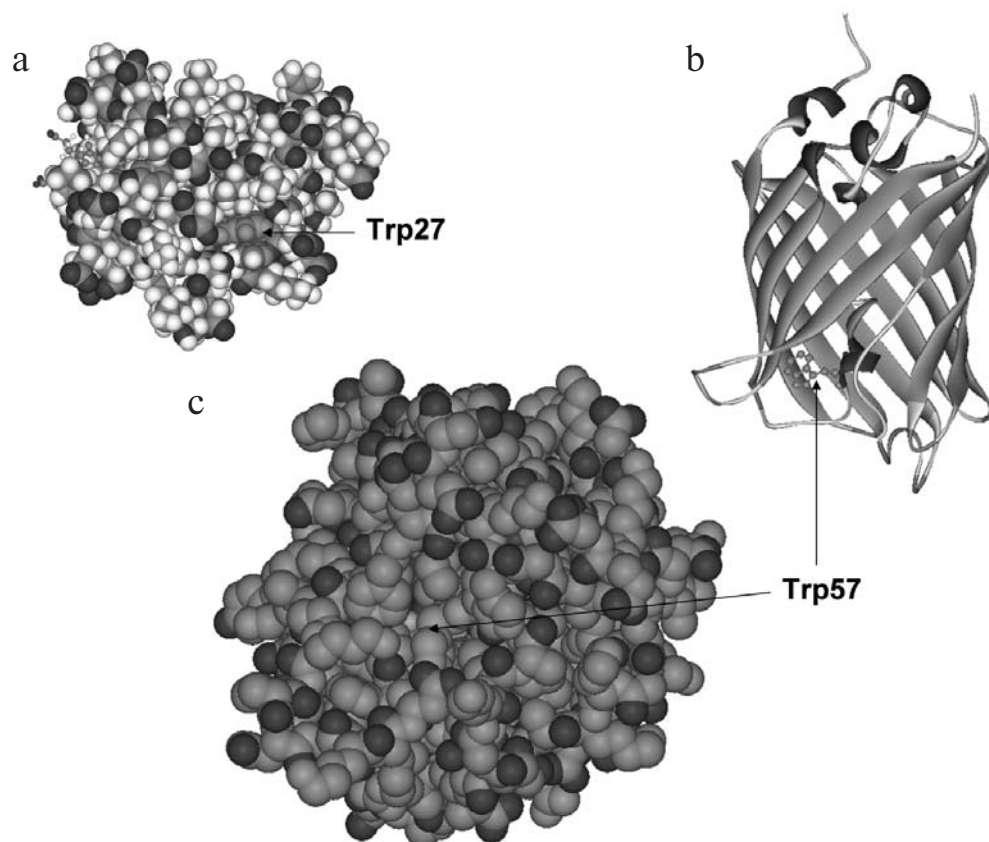
**Table 2.** Stern–Volmer constants for tryptophan residue fluorescence quenching in native and denatured forms of cytochrome *b*<sub>5</sub>, EGFP, and fusion protein Hmwb<sub>5</sub>–EGFP by acrylamide, I<sup>−</sup>, and Cs<sup>+</sup>

Protein	Wavelength, nm	Acrylamide		I <sup>−</sup>		Cs <sup>+</sup>	
		I	II	I	II	I	II
Cytochrome <i>b</i> <sub>5</sub>	331	2.76 ± 0.04	5.4 ± 0.2	0.71 ± 0.02	2.72 ± 0.08	7.5 ± 0.5	13.3 ± 0.7
	350	3.1 ± 0.4	6.2 ± 0.1	1.2 ± 0.1	3.5 ± 0.1	8.1 ± 0.5	13.6 ± 0.6
EGFP	331	4.41 ± 0.4	7.3 ± 0.3	1.33 ± 0.03	3.5 ± 0.3	7.9 ± 0.7	13.5 ± 0.6
	350	4.5 ± 0.3	8.56 ± 0.4	1.4 ± 0.4	14.2 ± 0.3	8.1 ± 0.3	3.8 ± 0.2
Hmwb <sub>5</sub> –EGFP	331	2.44 ± 0.04	5.3 ± 0.4	0.69 ± 0.03	3.4 ± 0.2	7.4 ± 0.6	12.3 ± 0.4
	350	3.2 ± 0.3	6.9 ± 0.3	1.1 ± 0.2	4.3 ± 0.5	7.5 ± 0.5	12.9 ± 0.6

Note: I, 20 mM K-P, pH 7.4; II, 20 mM K-P, 6 M GuHCl, pH 7.4.

rescence spectroscopy for cytochrome *b*<sub>5</sub>, one of the forms of green fluorescent protein, as well as their fusion protein. The rate constants of concentration-dependent dynamic quenching of tryptophan residue fluorescence for all three of these proteins were determined and ther-

modynamic parameters describing the process of protein globule unfolding for the free molecules as well as for the individual domains in the structure of fusion protein were obtained. It is shown for the first time that stability of individual components of a fusion protein can be signifi-

**Fig. 6.** Localization and exposure to solvent of Trp27 of the hydrophilic domain of cytochrome *b*<sub>5</sub> (pdb code 1AW3) (a); tertiary structure (b), localization and exposure to solvent (c) of the Trp57 residue of green fluorescent protein (pdb code 2QU1).

cantly different from the stability of separate proteins in solution. We think the main reason for this phenomenon might be steric effects arising due to small length of linker connecting the two globular proteins, which limits the freedom of conformational mobility of the constituent proteins. Further studies of artificially created and naturally occurring multidomain proteins will undoubtedly clarify these regularities in more detail.

## REFERENCES

- Gilep, A. A., Guryev, O. L., Usanov, S. A., and Estabrook, R. W. (2001) *Biochem. Biophys. Res. Commun.*, **284**, 937-941.
- Gilep, A. A., Guryev, O. L., Usanov, S. A., and Estabrook, R. W. (2001) *Arch. Biochem. Biophys.*, **390**, 222-234.
- Gilep, A. A., Guryev, O. L., Usanov, S. A., and Estabrook, R. W. (2001) *Arch. Biochem. Biophys.*, **390**, 215-221.
- Munro, A. W., Lindsay, J. G., Coggins, J. R., Kelly, S. M., and Price, N. C. (1996) *Biochim. Biophys. Acta*, **1296**, 127-137.
- Eiben, S., Bartelmas, H., and Urlacher, V. B. (2007) *Appl. Microbiol. Biotechnol.*, **75**, 1055-1061.
- Vergeres, G., and Waskell, L. (1995) *Biochimie*, **77**, 604-620.
- Schenkman, J. B., and Jansson, I. (2003) *Pharmacol. Ther.*, **97**, 139-152.
- Vergeres, G., Ramsden, J., and Waskell, L. (1995) *J. Biol. Chem.*, **270**, 3414-3422.
- Kozutsumi, Y., Kawano, T., Yamakawa, T., and Suzuki, A. (1990) *J. Biochem.*, **108**, 704-706.
- Hultquist, D. E., and Passon, P. G. (1971) *Nat. New Biol.*, **229**, 252-254.
- Takematsu, H., Kawano, T., Koyama, S., Kozutsumi, Y., Suzuki, A., and Kawasaki, T. (1994) *J. Biochem.*, **115**, 381-386.
- Hildebrandt, A., and Estabrook, R. W. (1971) *Arch. Biochem. Biophys.*, **143**, 66-79.
- Hlavica, P. (1984) *Arch. Biochem. Biophys.*, **228**, 600-608.
- Porter, T. D. (2002) *J. Biochem. Mol. Toxicol.*, **16**, 311-316.
- Guryev, O., Carvalho, R. A., Usanov, S., Gilep, A., and Estabrook, R. W. (2003) *Proc. Natl. Acad. Sci. USA*, **100**, 14754-14759.
- Guryev, O. L., Gilep, A. A., Usanov, S. A., and Estabrook, R. W. (2001) *Biochemistry*, **40**, 5018-5031.
- Yamazaki, H., Shimada, T., Martin, M. V., and Guengerich, F. P. (2001) *J. Biol. Chem.*, **276**, 30885-30891.
- Yantsevich, A. V., Harnostai, I. N., Lukashevich, O. P., Gilep, A. A., and Usanov, S. A. (2007) *Biochemistry (Moscow)*, **72**, 77-83.
- Porath, J., and Olin, B. (1983) *Biochemistry*, **22**, 1621-1630.
- Chudaev, M. V., and Usanov, S. A. (1997) *Biochemistry (Moscow)*, **62**, 401-411.
- Tsien, R. Y. (1998) *Annu. Rev. Biochem.*, **67**, 509-544.
- Laemmli, U. K. (1970) *Nature*, **227**, 680-685.
- Pace, C. N. (1986) *Meth. Enzymol.*, **131**, 266-280.
- Eftink, M. R. (1998) *Biochemistry (Moscow)*, **63**, 276-284.
- Pfeil, W. (1981) *Mol. Cell Biochem.*, **40**, 3-28.
- Manyusa, S., Mortuza, G., and Whitford, D. (1999) *Biochemistry*, **38**, 14352-14362.
- Manyusa, S., and Whitford, D. (1999) *Biochemistry*, **38**, 9533-9540.
- Pfeil, W. (1993) *Protein Sci.*, **2**, 1497-1501.
- Huang, J. R., Craggs, T. D., Christodoulou, J., and Jackson, S. E. (2007) *J. Mol. Biol.*, **370**, 356-371.
- Andrews, B. T., Gosavi, S., Finke, J. M., Onuchic, J. N., and Jennings, P. A. (2008) *Proc. Natl. Acad. Sci. USA*, **105**, 12283-12288.